

On the consistency of the expansion with the perturbations

Radouane Gannouji¹ and David Polarski²

¹*Instituto de Física, Pontificia Universidad Católica de Valparaíso, Casilla 4950, Valparaíso, Chile*

²*Laboratoire Charles Coulomb, Université Montpellier 2 & CNRS UMR 5221, F-34095 Montpellier, France*

Assuming a simple form for the growth index $\gamma(z)$ depending on two parameters $\gamma_0 \equiv \gamma(z=0)$ and $\gamma_1 \equiv \gamma'(z=0)$, we show that these parameters can be constrained using *background* expansion data. We explore systematically the preferred region in this parameter space. Inside General Relativity we obtain that models with a quasi-static growth index and $\gamma_1 \approx -0.02$ are favoured. We find further the lower bounds $\gamma_0 \gtrsim 0.53$ and $\gamma_1 \gtrsim -0.15$ for models inside GR. Models outside GR having the same background expansion as Λ CDM and arbitrary $\gamma(z)$ with $\gamma_0 = \gamma_0^{\Lambda\text{CDM}}$, satisfy $G_{\text{eff},0} > G$ for $\gamma_1 > \gamma_1^{\Lambda\text{CDM}}$, and $G_{\text{eff},0} < G$ for $\gamma_1 < \gamma_1^{\Lambda\text{CDM}}$. The first models will cross downwards the value $G_{\text{eff}} = G$ on very low redshifts $z < 0.3$, while the second models will cross upwards $G_{\text{eff}} = G$ in the same redshift range. This makes the realization of such modified gravity models even more problematic.

I. INTRODUCTION

Understanding the origin of the present accelerated expansion of the universe remains a challenge for theorists. A huge number of theoretical models and mechanisms were suggested and investigated that can produce this late-time accelerated expansion, see the reviews [1]. It is remarkable that the simplest model where gravity is described by General Relativity (GR) containing a cosmological constant Λ offers broad consistency with existing data, especially on large cosmic scales. While deriving the tiny value of Λ from first principles using quantum field theory still remains an outstanding problem, the phenomenological agreement of this model with observations provides a benchmark for the assessment of other proposed dark energy (DE) models.

An efficient way to make progress is to carefully explore the phenomenology of the proposed models and to compare it with observations [2]. Hence it is important to find tools which can efficiently discriminate between models, or between classes of models (e.g. [3]). The growth index γ , which gives a way to parametrize the growth of density perturbations of the non-relativistic matter (dust) component is an interesting example of such a phenomenological tool. This approach was pioneered long ago in order to discriminate spatially open from spatially flat universes [4] and then generalized to other cases [5]. It was revived recently in the context of dark energy models [6] and it has been investigated and used in various disguise (see e.g. [7]). As it is the case with many other quantities of interest, we can expect a significant improvement of the measurement of γ in the future thereby providing new observational constraints on DE models. A crucial property is that the growth index has a clear signature when DE reduces to a cosmological constant Λ : the growth index at very low redshifts lies around 0.55 and it is quasi-constant. This behaviour can be extended to noninteracting DE models inside GR with a constant (or even smoothly varying) equation of state w_{DE} , while a strictly constant γ is very peculiar [8]. Such behaviour is strongly violated in some

models beyond GR, see e.g. [9, 10] offering therefore the additional possibility to single out DE models formulated outside GR.

To constrain DE models, one can use the consistency of the background expansion with the matter perturbations growth. The growth index is just one of the phenomenological tools for the study of matter perturbations. There are several ways in which it can be used in order to constrain DE models. One can assume some DE model and study the behaviour of the growth index together with the possible background expansions. Then the behaviour of γ which is found expresses automatically the consistency mentioned above. Another way to exploit this consistency is by reconstructing the background expansion using the perturbations for a given class of DE models, a property emphasized some time ago [11]. In principle, even inside GR, it requires the knowledge of the perturbation functions $\delta_m(z)$, and of some additional cosmological parameters, in order to reconstruct $H(z)$. So an exact reconstruction is generally a complicated problem.

As we will show however, the growth index provides a very effective tool in this respect too. Actually, the reconstruction of $h(z) \equiv \frac{H(z)}{H_0}$ was given in [12] for a constant γ inside GR. Here, we will extend this result to more general behaviours of $\gamma(z)$. We will further extend this approach to modified gravity DE models and reconstruct the (effective) gravitational constant. It is this use of the growth index that we address in the present work.

II. THE GROWTH INDEX

We recall briefly the basic equations and concepts concerning the growth index. We consider a spatially flat Friedmann-Lemaître-Robertson-Walker (FLRW) universe filled with standard dust-like matter and DE components. We can neglect radiation in the matter and DE dominated stages. Deep inside the Hubble radius, the evolution of linear scalar (density) perturbations $\delta_m = \delta\rho_m/\rho_m$ in the (dust-like) matter compo-

ment follows from the equation (for GR)

$$\ddot{\delta}_m + 2H\dot{\delta}_m - 4\pi G\rho_m\delta_m = 0, \quad (1)$$

where $H(t) \equiv \dot{a}(t)/a(t)$ is the Hubble parameter and $a(t)$ is the scale factor, while G is Newton's gravitational constant. The evolution of the Hubble parameter as a function of the redshift $z = \frac{a_0}{a} - 1$ at $z \ll z_{eq}$ reads

$$h^2(z) = \Omega_{m,0}(1+z)^3 + (1 - \Omega_{m,0})e^{3 \int_0^z \frac{1+w_{DE}(z')}{1+z'} dz'} \quad (2)$$

with $h(z) \equiv \frac{H}{H_0}$ and $w_{DE}(z) \equiv p_{DE}(z)/\rho_{DE}(z)$. Equation (2) holds for all non-interacting DE models inside GR. We have the useful relation $w_{DE} = \frac{1}{3(1-\Omega_m)} \frac{d \ln \Omega_m}{d \ln a}$ using the standard definition $\Omega_m = \Omega_{m,0} \left(\frac{a_0}{a}\right)^3 h^{-2}$.

Instead of δ_m , it may be convenient to introduce the growth function $f \equiv \frac{d \ln \delta_m}{d \ln a}$. Then (1) leads to the following nonlinear first order equation [13]

$$\frac{df}{dN} + f^2 + \frac{1}{2} \left(1 - \frac{d \ln \Omega_m}{dN}\right) f = \frac{3}{2} \Omega_m, \quad (3)$$

with $N \equiv \ln a$. The quantity δ_m is easily recovered from f , viz.

$$\delta_m(a) = \delta_{m,i} \exp \left[\int_{a_i}^a f(x') \frac{dx'}{x'} \right]. \quad (4)$$

Obviously $f = p$ for $\delta_m \propto a^p$ (with p constant). In particular $f \rightarrow 1$ in Λ CDM for large z and $f = 1$ in the Einstein-de Sitter universe. In order to characterize the growth of perturbations, the parametrization $f = \Omega_m(z)^\gamma$ has been intensively used and investigated in the context of dark energy, where γ is the growth index. In general however, γ is not constant and one should write

$$f = \Omega_m(z)^{\gamma(z)}. \quad (5)$$

Surprisingly, it turns out that the growth index is quasi-constant for Λ CDM. Such a behaviour holds also for smooth non-interacting DE models inside GR when w_{DE} is constant [8]. It is known however that this behaviour changes substantially in modified gravity, an important motivation for the use of the growth index in the study of DE. In many DE models outside GR the dynamics of matter perturbations is modified by the replacement $G \rightarrow G_{\text{eff}}$ in (1), see e.g. [14], where G_{eff} is a model-dependent effective gravitational coupling. Introducing the quantity

$$g \equiv \frac{G_{\text{eff}}}{G}, \quad (6)$$

we obtain instead of Eq. (3)

$$\frac{df}{dN} + f^2 + \frac{1}{2} \left(1 - \frac{d \ln \Omega_m}{dN}\right) f = \frac{3}{2} g \Omega_m. \quad (7)$$

which can be recast into

$$2 \ln \Omega_m \frac{d\gamma}{dN} + (2\gamma - 1) \frac{d \ln \Omega_m}{dN} + 1 + 2\Omega_m^\gamma - 3g\Omega_m^{1-\gamma} = 0. \quad (8)$$

Note that in (7), (8), the cosmological parameters $\Omega_i = \frac{8\pi G\rho_i}{3H^2}$ are defined as in GR i.e. using Newton's gravitational constant G . We also see a degeneracy which can be read from equation (8). In fact, we can have an infinite number of combinations (g, γ) which produce the same Ω_m as for example in Λ CDM. It is interesting that G_{eff} can be constructed in an algebraic way once the background and the linear perturbations are measured with enough precision. Note that G_{eff} can also be scale dependent in modified gravity models with screening of a fifth force on small scales. This in turn induces a scale dependence of γ . In that case all equations and results hold for each scale separately. In this work we will consider a growth index which is essentially scale independent. From (7) one gets the following equality

$$w_{DE} = -\frac{1}{3(2\gamma - 1)} \frac{2 \frac{d\gamma}{dN} \ln \Omega_m + 1 + 2\Omega_m^\gamma - 3g\Omega_m^{1-\gamma}}{1 - \Omega_m} \quad (9)$$

$$\equiv -\frac{1}{3(2\gamma - 1)} \left[\frac{2 \frac{d\gamma}{dN} \ln \Omega_m}{1 - \Omega_m} + F(\Omega_m, \gamma, g) \right]. \quad (10)$$

which expresses the essential physical content of our formalism. The last expression defines the quantity $F(\Omega_m, \gamma, g)$ which encodes the dependence of w_{DE} on Ω_m for constant γ . The case $g = 1$ reduces to GR. We refer to [12] for additional details.

III. RECONSTRUCTION

The basic formalism outlined in the previous section allows for a reconstruction program in various ways. If we include modified gravity DE models, we have three unknown functions $h(z)$, $\gamma(z)$ and $g(z)$ in (8). Fixing two of these functions, or making reasonable assumptions, one can reconstruct the third unknown function.

A. Reconstruction of the background expansion inside GR

Let us consider first DE models where gravity is described by GR ($g = 1$). As noted some time ago, it is interesting that the background expansion can be reconstructed from the matter perturbations [11]. Hence knowing both the expansion and the perturbations growth one can check the consistency of a given model. As it was emphasized in [12], for non-interacting DE models, when the growth index γ is constant, this mathematical property reduces to the fact that all background quantities can be expressed in parametric form using the variable Ω_m . One obtains in particular [12] from (8) for constant γ

$$\ln(1+z) = (2\gamma - 1) \int_{\Omega_{m,0}}^{\Omega_m} \frac{d \ln \Omega_m}{1 + 2\Omega_m^\gamma - 3\Omega_m^{1-\gamma}}. \quad (11)$$

The cosmic time t can be expressed in a similar way [12]. From (11), one can recover $h(z)$ and reconstruct therefore the background expansion.

This result can be extended to a larger number of models for which the growth index is not exactly constant. Indeed, even in this case it is still possible to find $\Omega_m(z)$ by solving the eq. (8). Clearly, this equation is useful only provided we know $\gamma(z)$ or at least if we can make simple assumptions concerning its behaviour. Ideally, it would be very useful if we can describe the functional dependence of $\gamma(z)$ with a limited set of parameters. We can write in full generality a Taylor expansion around its value today, viz.

$$\gamma = \gamma_0 + \gamma_1 (1-x) + \gamma_2 (1-x)^2 + \dots \quad (12)$$

$$= \gamma_0 + \gamma_1 \frac{z}{1+z} + \gamma_2 \left(\frac{z}{1+z}\right)^2 + \dots \quad (13)$$

with $x \equiv \frac{a}{a_0}$. Obviously, it is desirable to have only two parameters when we derive observational constraints. Hence, instead of (13) we will use the more tractable representation

$$\gamma = \gamma_0 + \gamma_1 (1-x). \quad (14)$$

On one hand, this choice is motivated by the fact that γ is quasi-constant for a large class of models inside GR, and for Λ CDM in the first place. For these models it is clear that accurate fits are obtained already with (14). Hence for these models, (14) provides a fit linear in a valid in the full range probed by the observations, and actually everywhere. This is in the same spirit as the CPL parametrization of the equation of state (EoS) parameter w_{DE} [15]. On the other hand, (14) holds for any model provided it is used on small enough redshifts.

Let us return to non interacting DE models with constant, or smoothly varying, w_{DE} . In that case, the behaviour of γ up to redshifts of a few is very well approximated with (14) (see e.g. [12]). For our purpose, we can make it more quantitative and we will say that a fit is good provided the reconstructed expansion is accurate. In other words, when the fit (14) is substituted in (8), with the *true* parameters γ_0 and γ_1 , the reconstructed $h(z)$ should be very close to the *true* function $h(z)$.

We illustrate our results with the fiducial Λ CDM model, see figure 1. The reconstruction of $h(z)$ turns out to be remarkably accurate already when the first order expansion (14) is used, with errors less than 0.2%. As we can see further from figure 1, it is interesting that inclusion of the next orders in the expansion barely improves the accuracy. Of course, this accuracy is not related to observational uncertainties.

To summarize, the expansion (14) up to first order provides a remarkably accurate reconstruction of the background expansion rate.

Actually, even the zeroth order, that is if we approximate γ by its present value γ_0 , gives a good reconstruction with a maximal error of about 2% only on the redshift range $0 \lesssim z \lesssim 3$. However an inaccurate reconstruction can easily lead to false conclusions. We see

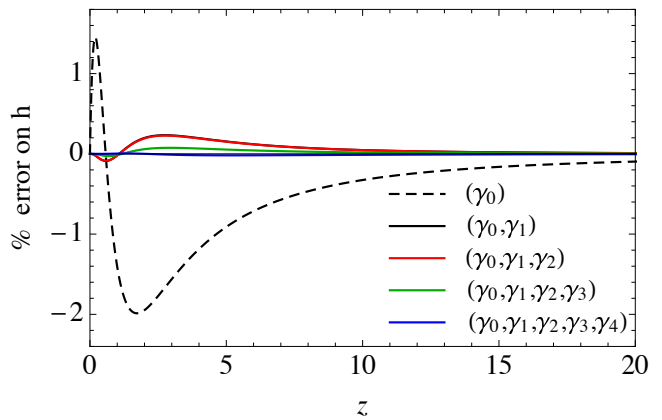


FIG. 1. The reconstructed relative Hubble function $h(z)$ is shown for our fiducial Λ CDM model with $\Omega_{m,0} = 0.30$ using $\gamma_0^{\Lambda CDM}$, $\gamma_1^{\Lambda CDM}$ in the expansion (14). Even the approximation $\gamma = \gamma_0^{\Lambda CDM}$ induces no more than a 2% error. With the first order expansion (14), the error reduces to about 0.2%. The expansion to first order (black) is hardly distinguishable from the second order expansion (red). Inclusion of higher order terms yields a marginal improvement in the accuracy.

from figure 1 that DE appears to be partly of the phantom type showing a “phantom-divide” crossing on some low redshift. Taken at face value it could lead to the conclusion that quintessence models are ruled out. Of course, this is because we have taken γ_0 and γ_1 corresponding to the peculiar case of Λ CDM so the slightest inaccuracy can lead to a phantom behaviour. When the first order expansion (14) is used, this phantom-divide crossing disappears essentially.

Our strategy is therefore simple: Each set (γ_0, γ_1) defines $\gamma(z)$ which, through eq.(8), gives in turn the background behaviour $\Omega_m(z)$ and therefore $h(z)$. This background can be compared to observations which will constrain the set of parameters (γ_0, γ_1) . Usually background data, are used to constrain cosmological background parameters like $\Omega_{m,0}$, $\Omega_{\Lambda,0}$ or $\Omega_{DE,0}$, and so on. Here, these data are used in order to explore in a systematic way the preferred region in the (γ_0, γ_1) parameter space characterizing the perturbations. In this section, we use the Pantheon data [16] consisting of 1048 type Ia supernovae (SNIa) covering the redshift range $0.01 < z < 2.3$, where we have marginalized χ^2 over the parameter H_0 , results are shown in Fig. 2. We can explore all points in the (γ_0, γ_1) plane around $(\gamma_0^{\Lambda CDM}, \gamma_1^{\Lambda CDM})$, for a given value of $\Omega_{m,0}$. We see from Fig. 2 that SNIa data favour a non constant γ which is slightly increasing in time. We also see that in a small range of the parameter space (γ_0, γ_1) non phantom evolution can occur in the range $0 \leq z \leq 1$. These points correspond to the triangular area displayed on figure 2. It is seen in particular that phantomness will always occur in this redshift range for $\gamma_0 < \gamma_0^{\Lambda CDM}$. Varying $\Omega_{m,0}$ will affect only marginally the shape of the triangle where phantomness is avoided.

By inspection of the expression for $h(z)$, we see that it

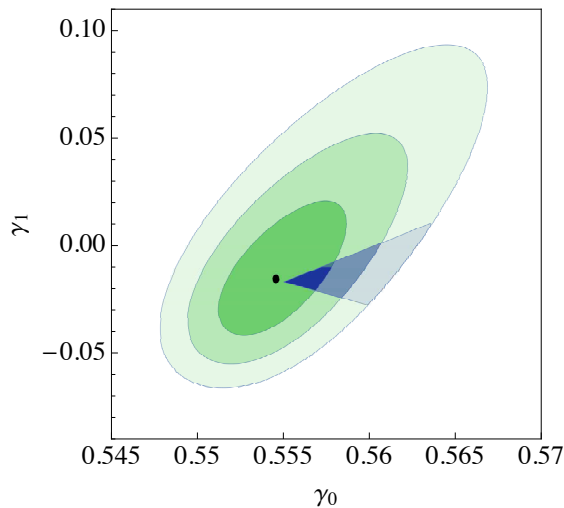


FIG. 2. The favoured region in the (γ_0, γ_1) plane is shown when GR is assumed ($g = 1$) and $\Omega_{m,0} = 0.3$ using SNIa data. The quantity γ_0 is rather sharply constrained at 2σ , $0.549 \lesssim \gamma_0 \lesssim 0.562$. In contrast, the constraint on γ_1 is much looser, $-0.06 \lesssim \gamma_1 \lesssim 0.05$. The best fit is $\gamma_0 = 0.555$ and $\gamma_1 = -0.016$. The dark triangular area represents those models which are not of the phantom type for $0 \leq z \leq 1$, the top left of the triangle corresponds to Λ CDM. We see in particular that for $\gamma_0 < \gamma_0^{\Lambda CDM}$ we get phantom DE for any value of γ_1 .

is completely fixed once the *background* parameter $\Omega_{m,0}$ and the EoS $w(z)$ are given. When $h(z)$ is reconstructed from the perturbations, we need the knowledge of $\Omega_{m,0}$, and $\gamma(z)$ and hence of γ_0 and γ_1 if (14) holds. In that sense, $\gamma(z)$ plays the same role as $w(z)$. Note that we can choose freely $\Omega_{m,0}$, γ_0 and γ_1 still satisfying

$$\gamma_1 = \frac{1 - \Omega_{m,0}}{2 \ln \Omega_{m,0}} \left[3w_0(2\gamma_0 - 1) + \frac{1 + 2\Omega_{m,0}^{\gamma_0} - 3\Omega_{m,0}^{1-\gamma_0}}{1 - \Omega_{m,0}} \right] \quad (15)$$

for $g(0) = 1$. While these results are interesting from a mathematical point of view, they imply an observational challenge when γ_1 is much smaller than γ_0 . In that case, it will be difficult to measure its value accurately in particular for models where it is at the level of $(1 - 2)\%$. In addition, if DE models have their γ_0 very close to each other, γ_0 would have to be measured with exquisite accuracy in order to differentiate these models observationally.

We also study the parameter space (γ_0, γ_1) by using cosmic chronometers, see Fig.3, using data compiled in [18–20]. While cosmic chronometers are presently less accurate than SNIa, they provide a promising way for a direct, essentially cosmology independent measurement of $H(z)$ [21] (see also e.g. [22]) and this is why we find it interesting to use them also, however separately. It is interesting that the confidence regions have different shapes in parameter space compared with the SNIa confidence regions. Finally, we compare the SNIa data to

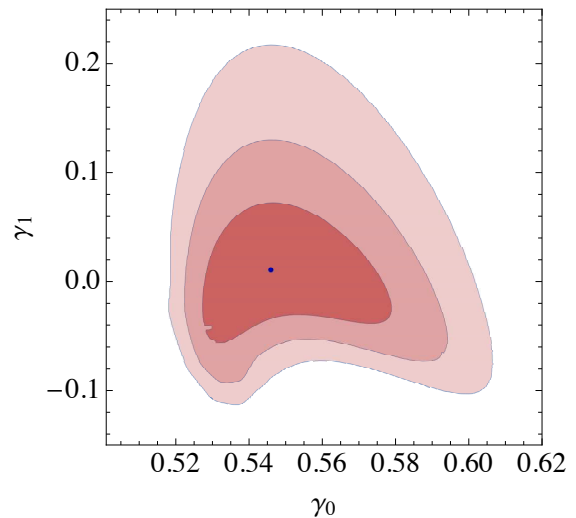


FIG. 3. The favoured region in the (γ_0, γ_1) plane is shown when GR is assumed ($g = 1$) and $\Omega_{m,0} = 0.3$ using cosmic chronometers. These probe directly $H(z)$ whence their importance. While the presently available data are less constraining, very different confidence regions are obtained compared to those resulting from SNIa data.

measurements of $f\sigma_8$ compiled in [23], see Fig.4. In that case too, SNIa data are much more constraining. Even if $f\sigma_8$ data provide less constraints on the parameter space (γ_0, γ_1) , we can see some sort of tension with SNIa and cosmic chronometers data. It is important to note, however, that only 17 data points are considered for $f\sigma_8$ data and because they are obtained for a fiducial cosmology, which is different in each survey, these data are thus rescaled by the Alcock-Paczinski factor [24] (see [25]). We stress that the constraints from $f\sigma_8$ data are likely to improve substantially in the future.

Considering all constraints, we see that as expected, the constraints on γ_0 are substantially tighter than on γ_1 . When using SNIa data, models having a quasi-static $\gamma(a)$ with $\gamma_1 \approx -0.02$ are favoured. While Λ CDM and noninteracting DE models with constant w_{DE} belong to the favoured models, the largest part of the preferred region corresponds to phantom DE on low redshifts. The preferred region at the 2σ level lies in the range $0.549 \lesssim \gamma_0 \lesssim 0.562$ for $\Omega_{m,0} = 0.3$. Interestingly, this corresponds essentially to the interval $-1.2 \lesssim w_{DE} \lesssim -0.8$ if a constant γ is assumed [12]. The parameter γ_1 lies in the range $-0.06 \lesssim \gamma_1 \lesssim 0.05$. Hence, while γ_0 is strongly constrained, larger variation of γ_1 is allowed. Remember that GR is assumed here.

We recall that these results depend on the assumed behaviour (14). We can try to derive results which are essentially model-independent by using data only on very small redshifts so that (14) now serves as a good fit. Though constraints necessarily become less stringent, conclusions drawn on the other hand are more general. We see from the lower panel of figure 5 that, at the 3σ confidence level, models with $\gamma_1 \lesssim -0.15$ or with

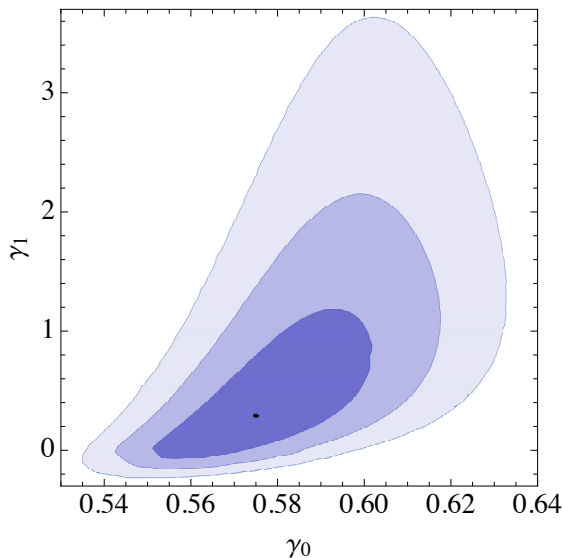


FIG. 4. The favoured region in the (γ_0, γ_1) plane is shown when GR is assumed ($g = 1$) using $f\sigma_8$ data. It is seen that the constraints *today* are substantially weaker than constraints coming from SNIa data (see Figure (2)).

$\gamma_0 \lesssim 0.53$ cannot be obtained inside GR. These results are in agreement with results obtained earlier for $f(R)$ models.

The constraints on γ_0 and γ_1 were obtained using the background expansion. As these data are expected to remain more accurate than perturbations data, so are the inferred constraints on γ_0 and γ_1 . We insist here again that the reconstructed function $h(z)$ is a genuine theoretical prediction. Another interesting aspect is connected to the value of H_0 . Indeed, γ_0 and γ_1 yield a reconstruction of $h(z)$, not of $H(z)$. Hence a pair γ_0 and γ_1 , and therefore the underlying model, can be in tension with $H(z)$ data, and even ruled out, depending on the H_0 value which is assumed. In our analysis we have chosen to marginalize the data over H_0 . The results of this subsection do not exclude the well-known possibility to distinguish models with significantly different γ_0 (and necessarily larger γ_1). Among the appealing cases where this can happen are modified gravity DE models to which we turn our attention now.

B. Reconstruction of g

We want to explore now another useful reconstruction. It was soon realized that a host of models are able to produce an accelerated expansion and even to produce an expansion rate close to that of Λ CDM. Hence, it is reasonable to assume some $h(z)$, which can later be refined as more accurate data will be released and to explore the possible behaviours of $\gamma(z)$, giving the matter perturbations, and of $g(z)$ which encodes the gravitational force driving these perturbations. We can use the ex-

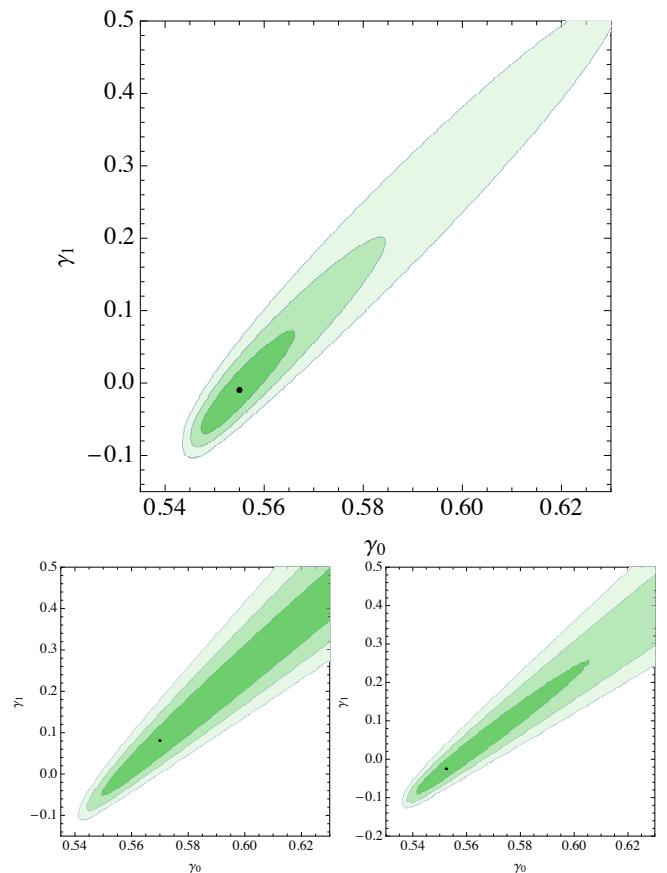


FIG. 5. The favoured region in the (γ_0, γ_1) plane is shown when GR is assumed ($g = 1$) and $\Omega_{m,0} = 0.3$ using data on very low redshifts. a) Upper panel: Pantheon SNIa data are used up to $z = 0.5$. Lower panel: SNIa data are used up to $z = 0.35$ for Pantheon data including systematics (on the left) and Union2.1 data [17] without systematics (on the right). On these low redshifts (14) is a good approximation and the constraints derived hold for all models. We see in particular the lower bounds $\gamma_0 \gtrsim 0.53$ and $\gamma_1 \gtrsim -0.15$.

pansion (13) up to first order around the present time which yields a good approximation on very low redshifts up to $z \lesssim (0.35 - 0.5)$. So we will assume a background evolving like Λ CDM and take γ given by (14). In this framework, we can reconstruct the evolution of $g(z)$, and this reconstruction will be accurate on all redshifts where (14) holds.

Once the background evolution is known and some ansatz is used for $\gamma(z)$, $g(z)$ is solved algebraically from (8). A first important point concerns the present-day value $g(0)$. Inspection of (8) shows that γ_1 contribute to its determination, raising its value for positive γ_1 and lowering it for negative γ_1 . On figure 6, points (γ_0, γ_1) corresponding to constant $g(0)$ are shown and it is seen that they correspond to straight lines. Any of these lines divide the plane in such a way that the domain on the left corresponds to a higher $g(0)$ while the domain on the right corresponds to a lower $g(0)$. Of particular importance is the line corresponding to $g(0) = 1$, for which the

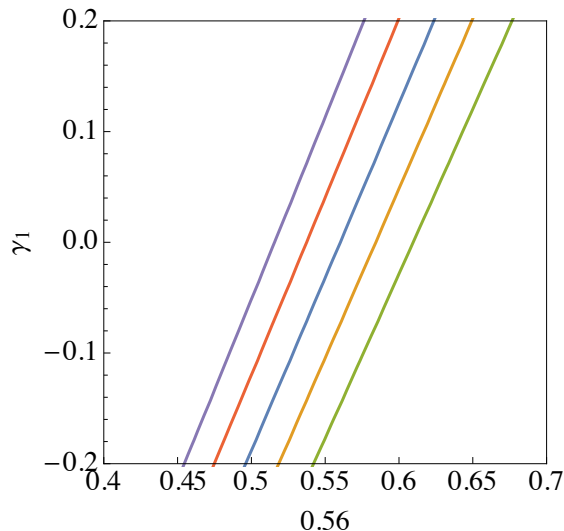


FIG. 6. The background is fixed to our fiducial Λ CDM model with $\Omega_{m,0} = 0.3$. From the left to the right, lines correspond to $g(0) = 1.2, 1.1, 1, 0.9, 0.8$. Points on the left, resp. on the right, of each line yield a higher, resp. lower, $g(0)$. Hence the line $g(0) = 1$ divides the plane in models with $g(0) > 1$ (upper part) and $g(0) < 1$ (lower part). Equivalently, if we fix the value of γ_0 , increasing, resp. decreasing, γ_1 will increase, resp. decrease, $g(0)$.

effective gravitational constant equals (the GR) Newton's constant G today. Modified gravity models that cannot allow for $g < 1$ are excluded from the domain on the right of this line.

However the subsequent behaviour for $z > 0$ can lead to a crossing of this line. Studying the behaviour of $g(z)$ in the (γ_0, γ_1) plane, still assuming a fixed Λ CDM background, we find the structure shown on figure 7.

The area around the point corresponding to Λ CDM can be divided into four regions. An inverted triangle is found above $(\gamma_0^{\Lambda CDM}, \gamma_1^{\Lambda CDM})$ where g started above one, $g(0) > 1$, and later satisfies $g(z) < 1$ at the redshift $z = 0.35$. Hence for points inside this triangle, the effective gravitational constant has crossed downwards the value G in the interval $0 < z < 0.35$. A similar triangle is found below $(\gamma_0^{\Lambda CDM}, \gamma_1^{\Lambda CDM})$ with the opposite behaviour, $g(0) < 1$ and $g(z) > 1$ at $z = 0.35$. In the remaining region on the left of $(\gamma_0^{\Lambda CDM}, \gamma_1^{\Lambda CDM})$ with $\gamma_0 < \gamma_0^{\Lambda CDM}$, one has $g > 1$ always up to $z = 0.35$, while in the remaining region on the right of $(\gamma_0^{\Lambda CDM}, \gamma_1^{\Lambda CDM})$ with $\gamma_0 > \gamma_0^{\Lambda CDM}$ we obtain $g < 1$ always up to $z = 0.35$. The left side of the upper triangle and the right side of the lower triangle represent those points for which $g = 1$ at $z = 0.35$. The line with the opposite sides of the triangles are those points starting with $g(0) = 1$.

We note here an interesting mathematical property. Assuming that our ansatz for $\gamma(z)$ holds for large z too, though we emphasize that this is generically not the case for modified gravity models, we can extend the figure for $z \rightarrow \infty$. As we move to higher redshifts, more and more models will cross the value $g = 1$, either downwards in the

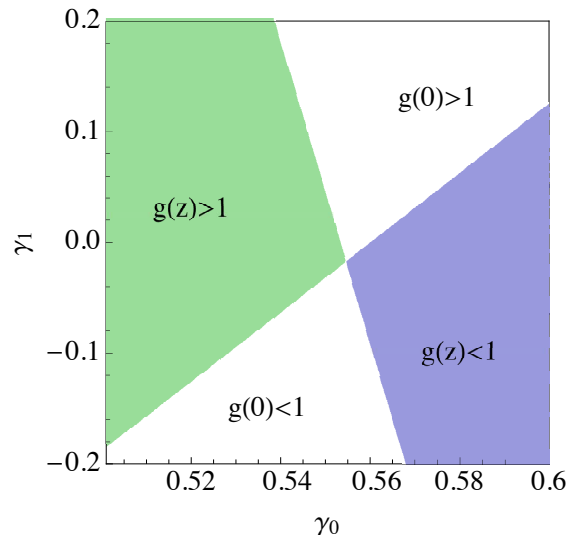


FIG. 7. The background is fixed to our fiducial Λ CDM model with $\Omega_{m,0} = 0.3$. Each pair γ_0, γ_1 represents a modified gravity DE model with fixed Λ CDM background evolution. The plane around $(\gamma_0^{\Lambda CDM}, \gamma_1^{(1),\Lambda CDM})$ is divided into four regions. To the left of $(\gamma_0^{\Lambda CDM}, \gamma_1^{(1),\Lambda CDM})$ are those models with $g(z) > 1$, to the right those with $g(z) < 1$. Models inside the upper (inverted) triangle start with $g(0) > 1$ and later cross the value $g = 1$ downwards for $z < 0.35$, models inside the lower triangle start with $g(0) < 1$ and cross $g = 1$ upwards for $z < 0.35$.

upper triangle, or upwards in the lower triangle. The left side of the upper triangle will move (counterclockwise) slightly to the left, and the right side of the lower triangle will move slightly to the right. The limit will be given by the line $\gamma_0 + \gamma_1 = \frac{6}{11}$. Indeed, the asymptotic behaviour of $g(z)$ for large z at arbitrary points in the (γ_0, γ_1) plane is given by

$$g(z) \sim 1 + \frac{1 - \Omega_{m,0}}{3\Omega_{m,0} z^3} [6 - 11(\gamma_0 + \gamma_1)] . \quad (16)$$

In the upper triangle we have $g \rightarrow 1$ from above, hence the last term in (16) tends to zero while positive; in the lower triangle we have the opposite situation and the last term of (16) tends to zero while negative. This is possible for $\gamma_0 + \gamma_1 = \frac{6}{11}$ only. Another way to see this is as follows. We know from theoretical considerations that the limit $\gamma_{-\infty} = \frac{6}{11}$ is obtained for Λ CDM in the asymptotic past [12]. However the line corresponding to $g = 1$ at $z \rightarrow \infty$ corresponds just to the Λ CDM model itself at $z \rightarrow \infty$, hence it must satisfy $\gamma_{-\infty} = \gamma_0 + \gamma_1 = \frac{6}{11}$.

Models with $\gamma_0 \approx \gamma_0^{\Lambda CDM}$ below the 1% level cannot be clearly differentiated from Λ CDM with measurements of γ_0 as long as γ_1 is not measured accurately, which can be expected for $|\gamma_1| \lesssim 0.05$. If we move along γ_0 to the right or to the left of $(\gamma_0^{\Lambda CDM}, \gamma_1^{\Lambda CDM})$, we get models with $g(0)$ departing moderately from 1 on very small redshifts, see right panel of figure 8. If we move

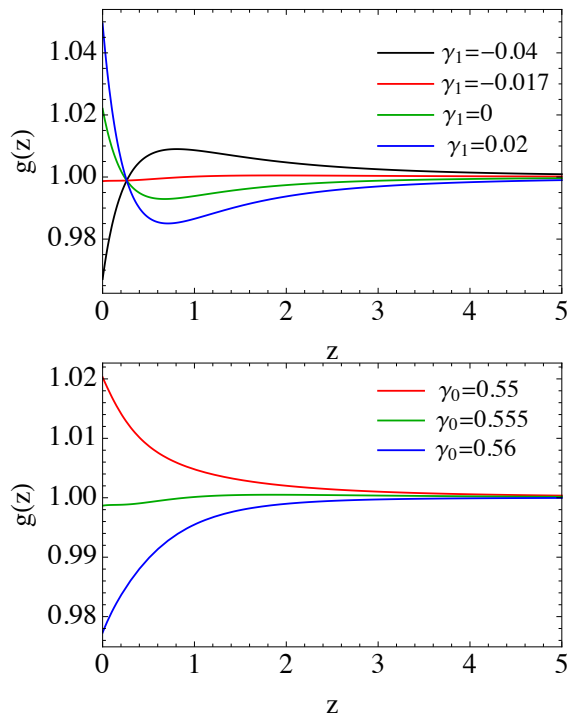


FIG. 8. a) The figure on the upper panel shows the behaviour of $g(z)$ when we move in the $\gamma_0 - \gamma_1$ plane above and below the fiducial Λ CDM model, $\gamma_0 = 0.555$, $\gamma_1 = -0.017$ and $\Omega_{m,0} = 0.3$. When we move upwards ($\gamma_1 > \gamma_1^{\Lambda CDM}$), resp. downwards ($\gamma_1 < \gamma_1^{\Lambda CDM}$), $g(0)$ increases, resp. decreases, and $g(z)$ crosses the value $g = 1$ at small redshifts. b) On the lower panel, the behaviour of $g(z)$ is shown when we move in the (γ_0, γ_1) plane to the left and to the right of our fiducial Λ CDM model. A moderate departure from $g = 1$ is obtained with $g > 1$, resp. $g < 1$, on the left, resp. right, of $\gamma_0^{\Lambda CDM}$.

upwards, resp. downwards, along γ_1 inside the upper, resp. lower, triangle, we have models mimicking Λ CDM for γ_1 not too large with $g(0)$ substantially higher, resp. lower than one. Those models however necessarily cross the value $g = 1$ at very low redshifts, hence they cannot be realized in models not allowing for such a crossing.

To summarize, models that cannot be distinguished observationally from Λ CDM through the measurement of γ_0 alone are mostly modified gravity models which can depart substantially from GR but which must necessarily allow for a crossing of $g = 1$ on small redshifts.

IV. CONCLUSIONS

A large family of noninteracting DE models inside GR, with Λ CDM among them, exhibits a quasi-constant be-

haviour of the growth index $\gamma(z)$. For these models, the behaviour (14) of $\gamma(z)$ can be expressed with two parameters only, namely γ_0 and γ_1 . It is then possible to reconstruct $h(z)$ for these models using the parameters γ_0 and γ_1 . Motivated by these examples, we have constrained systematically the two parameters γ_0 and γ_1 using background expansion data for all models satisfying (14) and we have found the preferred region in the (γ_0, γ_1) plane. We have obtained that while γ_0 is rather tightly constrained around $\gamma_0^{\Lambda CDM}$, a large range remains for the parameter γ_1 . Such an accuracy could not be obtained using perturbations data in view of the large errors on the growth function f . We have refined our analysis by using background data on very small redshifts, so that the assumed behaviour (14) becomes a good approximation for all (reasonable) models. We find in particular that γ_0 and γ_1 are bounded from below. Values measured below these bounds, and such models were found earlier, would hint at either modified gravity (see e.g. [26],[27]) or interacting DE models (see e.g. [28, 29]).

We have also considered DE modified gravity models assuming a fixed fiducial background dynamics, Λ CDM in our analysis. Though a quasi-constant behaviour for $\gamma(z)$ cannot be assumed in this case, it can be used on very small redshifts, in the important range where DE is expected to induce the universe present accelerated expansion. We have investigated modified gravity models which cannot be discriminated from Λ CDM as a result of large errors on the parameter γ_1 while observations are able to pinpoint the value of γ_0 below the 1% level. Though some investigated modified gravity models yield a significantly lower γ_0 , we study here the price to pay for modified gravity models in order to satisfy $\gamma_0 \approx \gamma_0^{\Lambda CDM}$. We have found that models with a substantial variation of the effective gravitational coupling today will cross Newtons constant G on very small redshifts, either upwards or downwards. This gives a very strong constraint, further restraining modified gravity models able to realize this phenomenology. For example, $f(R)$ DE models do not allow for such a behaviour though this is possible in other models [30]. As the goal of future experiments will be to probe the growth index and a possible departure from GR, a systematic study of the consistency of the background expansion with the perturbations along the lines presented in this work can give interesting phenomenological constraints as well as new insights.

ACKNOWLEDGMENTS

The authors thank Benjamin L’Huillier for many helpful comments and for sharing with us compiled $f\sigma_8$ data used in this paper. The work of R. Gannouji is supported by Fondecyt project No 1171384.

[1] V. Sahni and A. A. Starobinsky, Int. J. Mod. Phys. D **9**, 373 (2000); P. J. E. Peebles and B. Ratra, Rev. Mod.

Phys. **75**, 559 (2003); E. J. Copeland, M. Sami and

- S. Tsujikawa, *Int. J. Mod. Phys. D* **15**, 1753 (2006); V. Sahni and A. A. Starobinsky, *Int. J. Mod. Phys.* **15**, 2105 (2006); M. Li, X.-D. Li, S. Wang and Y. Wang, *Commun. Theor. Phys.* **56**, 525 (2011).
- [2] D. H. Weinberg, M. J. Mortonson, D. J. Eisenstein, C. Hirata, A. G. Riess and E. Rozo, *Phys. Rept.* **530**, 87 (2013); L. Amendola *et al.*, *Living Rev. Rel.* **16**, 6 (2013); P. Bull *et al.*, *Phys. Dark Univ.* **12**, 56 (2016).
- [3] V. Sahni, A. Shafieloo and A. A. Starobinsky, *Astrophys. J.* **793**, L40 (2014); A. Shafieloo, B. L'Huilier and A. A. Starobinsky, [arXiv:1804.04320].
- [4] P. J. E. Peebles, *Astrophys. J.* **284**, 439 (1984).
- [5] O. Lahav, P. B. Lilje, J. R. Primack and M. J. Rees, *MNRAS* **251**, 128 (1991).
- [6] E. V. Linder and R. N. Cahn, *Astropart. Phys.* **28** 481 (2007).
- [7] M. Malekjani, S. Basilakos, Z. Davari, A. Mehrabi, M. Rezaei, *Mon. Not. Roy. Astron. Soc.* **464**, 1192 (2017); Alberto Bailoni, Alessio Spurio Mancini, Luca Amendola, arXiv:1608.00458; Xiao-Wei Duan, Min Zhou, Tong-Jie Zhang, arXiv:1605.03947; N. Nazari-Pooya, M. Malekjani, F. Pace, D. Mohammad-Zadeh Jassur, *Mon. Not. Roy. Astron. Soc.* **458**, no.4, 3795 (2016); S. Basilakos, J. Solà, *Phys. Rev. D* **92**, no.12, 123501 (2015); I. de Martino, M. De Laurentis, S. Capozziello, *Universe* **1**, no. 2, 123 (2015); J. N. Dossett, M. Ishak, D. Parkinson, T. Davis, *Phys.Rev. D* **92**, no.2, 023003 (2015); A. B. Mantz *et al.*, *Mon. Not. Roy. Astron. Soc.* **446**, 2205 (2015); S. Nesseris, S. Basilakos, E.N. Saridakis, L. Perivolaropoulos, *Phys. Rev. D* **88** 103010 (2013); K. Bamba, Antonio Lopez-Revelles, R. Myrzakulov, S.D. Odintsov, L. Sebastiani, *Class. Quant. Grav.* **30** 015008 (2013); A. Bueno belloso, J. Garcia-Bellido, D. Sapone, *JCAP* **1110**, 010 (2011); R. Bean, M Tangmatitham, *Phys. Rev. D* **81**, 083534 (2010); Puxun Wu, Hong Wei Yu, Xiangyun Fu, *JCAP* **0906**, 019 (2009); Seokcheon Lee, Kin-Wang Ng, *Phys. Lett.* **B688**, 1 (2010); Yungui Gong, *Phys.Rev. D* **78**, 123010 (2008); V. Acquaviva, A. Hajian, D. N. Spergel, S. Das, *Phys. Rev. D* **78** 043514 (2008); Hao Wei, *Phys. Lett.* **B664** 1 (2008); S. Nesseris, L. Perivolaropoulos, *Phys. Rev. D* **77**, 023504 (2008).
- [8] D. Polarski and R. Gannouji, *Phys. Lett. B* **660**, 439 (2008).
- [9] R. Gannouji, B. Moraes and D. Polarski, *JCAP* **0902**, 034 (2009).
- [10] H. Motohashi, A. A. Starobinsky and J. Yokoyama, *Progr. Theor. Phys.* **123**, 887 (2010).
- [11] A. A. Starobinsky, *JETP Lett.* **68**, 757 (1998) [arXiv:astro-ph/9810431].
- [12] D. Polarski, A. A. Starobinsky and H. Giacomini, *JCAP* **1612**, 037 (2016).
- [13] L. Wang and P. J. Steinhardt, *Astrophys. J.* **508**, 483 (1998).
- [14] B. Boisseau, G. Esposito-Farèse, D. Polarski and A. A. Starobinsky, *Phys. Rev. Lett.* **85**, 2236 (2000).
- [15] M. Chevallier and D. Polarski, *Int. J. Mod. Phys. D* **10**, 213 (2001); E. V. Linder, *Phys. Rev. Lett.* **90**, 091301 (2003).
- [16] D. M. Scolnic *et al.*, *Astrophys. J.* **859** (2018) no.2, 101 doi:10.3847/1538-4357/aab9bb [arXiv:1710.00845 [astro-ph.CO]].
- [17] N. Suzuki *et al.*, *Astrophys. J.* **746** (2012) 85 doi:10.1088/0004-637X/746/1/85 [arXiv:1105.3470 [astro-ph.CO]].
- [18] H. Yu, B. Ratra and F. Y. Wang, *Astrophys. J.* **856** (2018) no.1, 3 doi:10.3847/1538-4357/aab0a2 [arXiv:1711.03437 [astro-ph.CO]].
- [19] S. Capozziello, R. D'Agostino and O. Luongo, doi:10.1093/mnras/sty422 arXiv:1712.04380 [astro-ph.CO].
- [20] A. Gómez-Valent and L. Amendola, *JCAP* **1804** (2018) no.04, 051 doi:10.1088/1475-7516/2018/04/051 [arXiv:1802.01505 [astro-ph.CO]].
- [21] R. Jimenez, A. Loeb, *Astrophys. J.* **573**, 37(2002).
- [22] M. Moresco, R. Jimenez, L. Verde, L. Pozzetti, A. Cimatti and A. Citro, [arXiv:1804.05864].
- [23] A. Shafieloo, B. L'Huilier and A. A. Starobinsky, arXiv:1804.04320 [astro-ph.CO].
- [24] C. Alcock and B. Paczynski, *Nature* **281** (1979) 358. doi:10.1038/281358a0
- [25] S. Nesseris, G. Pantazis and L. Perivolaropoulos, *Phys. Rev. D* **96** (2017) no.2, 023542 doi:10.1103/PhysRevD.96.023542 [arXiv:1703.10538 [astro-ph.CO]].
- [26] T. Clifton, P. G. Ferreira, A. Padilla and C. Skordis, *Phys. Rept.* **513**, 1 (2012); A. Joyce, B. Jain, J. Khoury and M. Trodden, *Phys. Rept.* **568**, 1 (2015).
- [27] L. Kazantzidis and L. Perivolaropoulos, [arXiv:1803.01337].
- [28] G. Caldera-Cabral, R. Maartens and B. M. Schaefer, *JCAP* **0907** (2009) 027 doi:10.1088/1475-7516/2009/07/027 [arXiv:0905.0492 [astro-ph.CO]].
- [29] B. Wang, E. Abdalla, F. Atrio-Barandela and D. Pavon, *Rept. Prog. Phys.* **79** (2016) no.9, 096901 doi:10.1088/0034-4885/79/9/096901 [arXiv:1603.08299 [astro-ph.CO]].
- [30] A. De Felice, L. Heisenberg, R. Kase, S. Mukohyama, S. Tsujikawa and Y. Zhang, *Phys. Rev. D* **94**, 044024 (2016).